IL NUOVO CIMENTO **46 C** (2023) 58
DOI 10.1393/ncc/i2023-23058-1

COMMUNICATIONS: SIF Congress 2022

Characterization of sensor modules for the CMS Barrel Timing Layer at HL-LHC

SIMONA PALLUOTTO([1])([2]) for the CMS COLLABORATION

([1]) *INFN, Sezione di Milano-Bicocca - Milano, Italy*
([2]) *Dipartimento di Fisica, Università degli Studi di Milano-Bicocca - Milano, Italy*

received 27 January 2023

Summary. — The CMS detector is undergoing an extensive upgrade program to prepare for the challenging conditions of the High-Luminosity LHC starting in 2029. In particular, a new timing detector will measure minimum ionizing particles with a time resolution of 30–60 ps. The technology selected for the central part of the detector, the Barrel Timing Layer, consists of scintillating crystals of lutetium yttrium oxyorthosilicate doped with cerium (LYSO:Ce) read out with silicon photomultipliers. A detailed characterization of several sensor modules, consisting of sixteen-channel crystal arrays coupled to a pair of Silicon Photomultiplier (SiPM) arrays, will be presented. The results represent the first thorough investigation of the performance of modules made with crystals and SiPMs of different geometries characterized with radioactive sources.

1. – Introduction

To extend its discovery potential, a High-Luminosity phase of the Large Hadron Collider (HL-LHC) featuring a nominal instantaneous luminosity of $5 \times 10^{34}\,\mathrm{cm}^{-2}\mathrm{s}^{-1}$ is scheduled to begin in 2029 and it is expected to deliver an integrated luminosity of $3000\,\mathrm{fb}^{-1}$ in about 10 years of operation. Experiments will increase their data sample by one order of magnitude compared with the LHC baseline program and they foresee exploring wide areas of research in terms of Standard Model (SM) precision measurements, study of the Higgs boson properties and searches of physics beyond the SM (BSM) [1]. Nevertheless, severe radiation damage to many of the existing detector components and a large number of spurious interactions per bunch crossing (pileup), *i.e.*, 200 pileup events to be compared to the current level of 40 at LHC, are envisaged to adversely affect the performances of detectors in reconstructing the collision events.

A dedicated timing layer has been designed for integration in the CMS detector [2]. The Minimum Ionizing Particle (MIP) Timing Detector (MTD) will provide CMS with

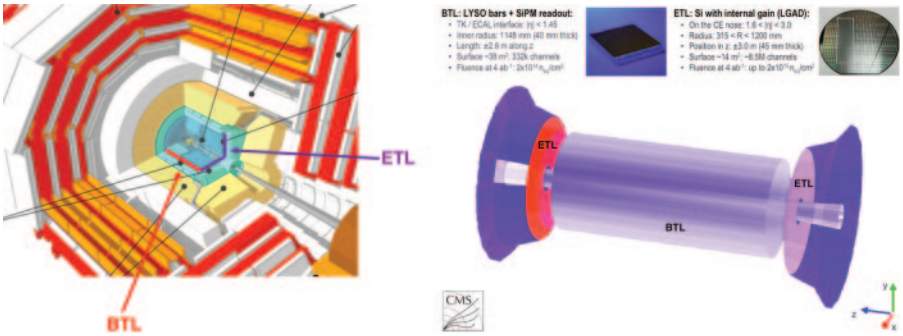

Fig. 1. – Left: a schematic representation of the current CMS design with its sub-detectors. Right: A representative view of the GEANT geometry of the MIP Timing Detector [3].

accurate measurements of the time of arrival of MIPs and it will face unparalleled challenges in terms of target time resolution and levels of radiation to withstand. Accurate timing measurements enable the use of 4-dimensional vertexing which improves the efficiency in reconstructing final-state observables (*e.g.*, isolated leptons, b-jets, etc.). The MTD will also bring new capabilities to CMS in identifying charged hadrons based on time of flight and it will consecutively yield benefits to studies such as Heavy Ion physics [3] and it will extend sensitivity to the study of BSM long-lived particles.

The MTD will equip both the barrel and the endcap part of CMS, as shown in fig. 1 and, since the Endcap Timing Layer (ETL) and the Barrel Timing Layer (BTL) will cover different pseudorapidity regions, they have to accomplish different requirements in terms of radiation tolerance. The ETL will be instrumented with Low-Gain Avalanche Detectors (LGADs), whereas the BTL sensors consist of elongated LYSO:Ce crystal bars readout at both ends by Silicon Photomultipliers (SiPMs). Each crystal bar has dimensions of about 57 mm in length and 3.12 mm in width. Depending on the pseudorapidity region, a variable thickness of 2.4, 3.0 or 3.75 mm, will maintain an approximately constant slant depth crossed by particles coming from the interaction point and will minimize the amount of material placed before the Electromagnetic Calorimeter. The crystal bar end faces and the SiPM active area are designed to feature the same width and the same thickness in order to optimize the Light Collection Efficiency (LCE), *i.e.*, the fraction of photons hitting the SiPM sensitive area of the overall number of photons initially produced. Each SiPM packaging is equipped with four Thermo-Electric Coolers (TECs) having the dimension of $3 \times 4\,\mathrm{mm}^2$. The implementation of such devices allows for further reducing the operating temperature and increasing the annealing temperature, thus mitigating the worsening of the timing performance due to radiation damage. A picture of a BTL module is reported in fig. 2.

The operation of BTL is based on the SiPMs detecting the scintillating photons produced by a MIP passing through the LYSO crystals. Time measurements are then extracted using a leading-edge discrimination of the pulses performed by a dedicated ASIC, the TOFHIR [4].

Since the publication of the MTD Technical Design Report in 2019, intense research has been focused on the finalization of the MTD design. In this study, potential strategies to enhance the BTL light output (LO), *i.e.*, the number of photons detected by the SiPMs in response to the passage of a MIP, and consecutively the timing capabilities,

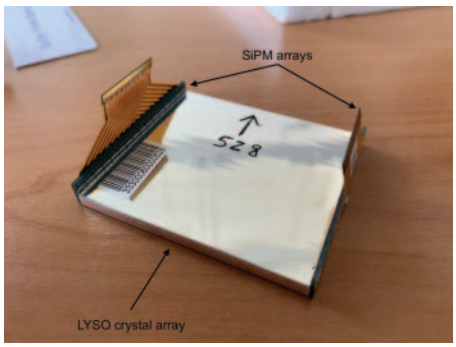

Fig. 2. – Picture of a BTL module. The LYSO array is glued at each side to a SiPM array.

were explored and comprehensive characterization of sensor modules of the barrel part of MTD is presented. This research was carried out along with the prototyping phase and it contributed in defining the final technical specifications of the BTL sensors.

2. – Motivations

The evolution of the BTL timing performance throughout HL-LHC was estimated through several simulation studies and it is shown in fig. 3.

The BTL time resolution may be degraded by several effects that introduce stochastic and systematic fluctuations and it can be expressed as

$$\sigma_t^{BTL} = \sigma_t^{clock} \oplus \sigma_t^{digi} \oplus \sigma_t^{ele} \oplus \sigma_t^{phot} \oplus \sigma_t^{DCR}. \tag{1}$$

The dominant contributions to the time resolution are the electronics noise, the photo-statistics and the Dark Count Rate (DCR) noise. The time fluctuations due to the digitization are assumed to be negligible (∼7 ps). The readout electronics in CMS is synchronised with the LHC bunch crossing and to be compliant with the time resolution requirements of the MTD, the clock distribution system must have less than 15 ps RMS link-to-link jitter over all clock distribution links.

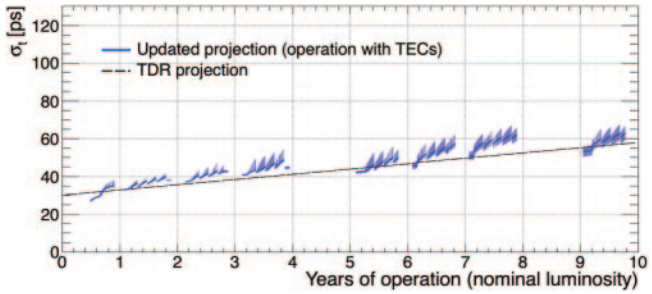

Fig. 3. – Projection of the timing performance of the BTL detector during the years of operation of HL-LHC. Both the TDR projections (black) and the latest projections (blue) including the annealing periods are reported.

The time jitter due to the electronics depends on the signal slew rate ($\mathrm{d}V/\mathrm{d}t$) that increases approximately linearly for larger signals [5]:

$$\sigma_t^{ele} \propto \frac{1}{\mathrm{d}V/\mathrm{d}t} \propto \frac{1}{N_{phe}}, \tag{2}$$

where N_{phe} is the amount of photoelectrons detected by the SiPM.

The photo-statistics term is due to the stochastic fluctuations in the time of arrival of photons detected at the SiPM and such contribution is estimated to be 25–30 ps. It can be expressed as

$$\sigma_t^{phot} \propto \sqrt{\frac{\tau_d}{N_{phe}}}, \tag{3}$$

where the time constant τ_d is referred to the decay time of the scintillation pulse that for the considered LYSO:Ce crystals is about 40 ns.

The increase in integrated luminosity during the operation of HL-LHC will induce radiation damage to the SiPMs creating defects in the material structure and generating dark counts whose magnitude depends on several factors such as the SiPM technology, the operating temperature and over-voltage, the annealing history which can cause a spontaneous recovery of the silicon defects. The radiation damage induced to the SiPMs generates an additional time jitter that is assumed to be negligible at the beginning of the operation of HL-LHC and it is estimated to be 50 ps after 3000 fb^{-1}. It can be expressed as

$$\sigma_t^{DCR} \propto \frac{\sqrt{DCR}}{N_{phe}}. \tag{4}$$

From eqs. (2), (3) and (4) it is clear that a key parameter to optimize the time resolution of the detector is the number of photoelectrons produced, N_{phe}, defined as

$$N_{phe} = LO \cdot PDE \cdot E_{dep} = LY \cdot LCE \cdot PDE \cdot E_{dep}, \tag{5}$$

where LO is the light output, PDE is the photon detection efficiency of the SiPM, E_{dep} is the energy deposited, LY is the light yield of the crystal, *i.e.*, the number of photons per MeV produced by the scintillation process inside the crystal, and LCE is the light collection efficiency of the detecting system.

In order to achieve the design goal and driven by the previous considerations, the main focus of this study was both to understand the parameters of the sensor modules that determine the light output and to explore various optimization possibilities.

3. – Module characterization

The measurements were performed in a laboratory in Milano-Bicocca where the experimental setup is housed inside a light-tight box with a controlled and actively stabilized temperature of $(22 \pm 1)^{\circ}$C. Since the SiPM functioning is strongly dependent on the temperature, it is crucial to carefully monitor it. The measurement of the light output of BTL modules was performed by normalizing the charge integral of SiPM pulses obtained by exposing the crystal bars to a radioactive ^{22}Na source to the charge corresponding

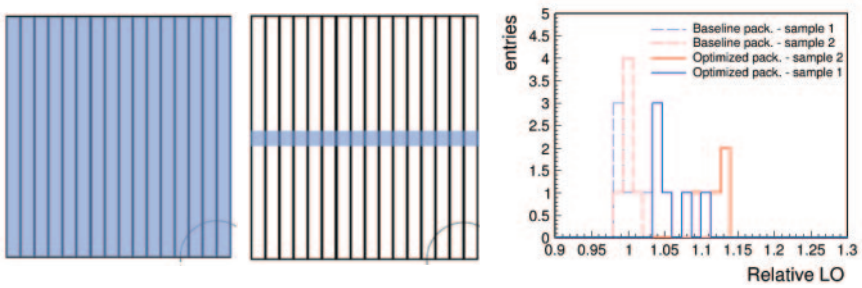

Fig. 4. – Left: pictorial comparison between the standard packaging (left) and the optimized packaging (middle). In both images, the blue area represents the glue deposition. Right: light output, normalized to the average light output measured with baseline packaging, for two samples from two different vendors.

to the single photoelectron. In particular, the impact of the LYSO array packaging, the SiPM resin protective layer and the sensor geometry on the LCE was studied and potential optimization strategies were investigated.

3˙1. *Impact of the LYSO array packaging*. – The light propagation inside the scintillator is influenced by the layer of wrapping materials covering the LYSO array and by the way it is attached to crystals. It also depends on the surface state of the crystal and on the probability for the photons to be absorbed inside the crystal or to escape from the lateral surfaces. Each LYSO vendor is responsible for the packaging of the crystal array which consists of a thin layer of wrapping material attached to the crystal array with a uniform layer of glue in order to provide more robust support to the array. An additional amount of glue is also used by most manufacturers between bars to further enhance mechanical robustness. Reducing the amount of glue on all crystal surfaces should result in an increase in internal reflection and an improvement in the light output of about 10%. Such potential enhancement of the LCE was therefore explored and the comparison between the two solutions is reported in fig. 4(left).

Crystal arrays with optimized packaging were purchased from different vendors. The modules with optimized packaging were characterized both in Rome and Milan and the corresponding results confirmed an average increase in the light output of 10% due to the new packaging. As an example, the results obtained for modules consisting of LYSO arrays from two different producers are reported in fig. 4(right). The expected improvement was therefore confirmed by these results and other studies on time resolution showed an improved performance. Due to these observations, the MTD Collaboration approved the optimized packaging for BTL modules.

3˙2. *Impact of the resin protective layer*. – Dedicated studies were focused on the impact of the SiPM protective window thickness on the LCE. The resin material and its thickness have an impact on the LCE: photons come out of a crystal bar with a wide angular distribution and, depending on the geometry of the sensor, only a fraction enters the active area of the SiPM corresponding to the bar where the light was produced. Besides, at the interface between the different media (resin-silicon), a fraction of the photons can be reflected and bounce back inside the resin thus being detected at a SiPM further away, as shown in fig. 5(left). The higher the number of photons that are detected

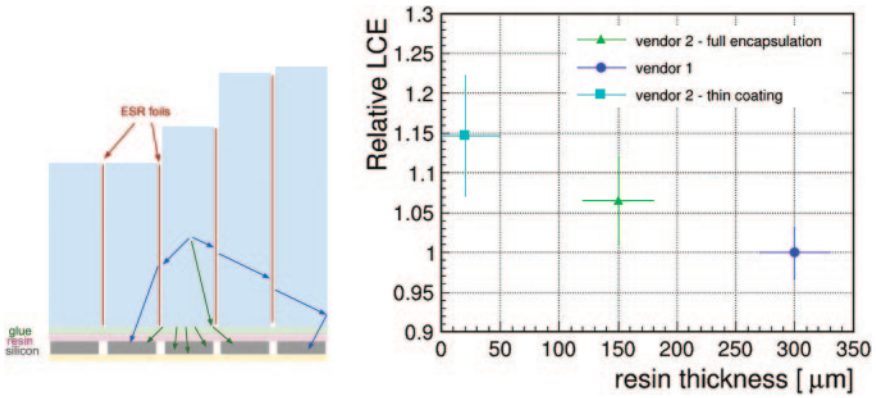

Fig. 5. – Left: pictorial representation of scintillating photons produced in a bar that manage to reach different SiPMs depending on their optical path. A fraction of the total amount of produced photons will be detected by the adjacent SiPMs to the considered SiPM. Right: relative light collection efficiency comparison between modules consisting of the same LYSO array coupled to SiPM arrays having different resin thicknesses.

by adjacent SiPMs, the smaller the light output measured in the crystal bar under test. Therefore, it is crucial to minimize this effect and consecutively its impact on the timing performance.

In particular, a SiPM vendor, later referred to as vendor 1, designed a new protective window featuring a thickness of 300 μm thick (blue marker in fig. 5(right)) and a refractive index of $n = 1.57$. The other vendor, referred to as vendor 2, proposed two different options: one consists of a full encapsulation of the SiPM made of a silicone resin 150 μm thick with $n = 1.41$ (green marker) and the other is a thin quartz layer deposition of 20 μm with $n = 1.56$ (light-blue marker).

The different solutions provided by the SiPM vendors for the protective windows allow for studying the impact of different materials and thicknesses of resin on the LCE and thus the LO. In particular, a LYSO array from a producer was coupled through optical grease to different SiPM arrays. A relative comparison between results of the light output measurements of such configurations is reported in fig. 5(right).

An improvement in LCE up to 15% was observed between the thin coated SiPM array from vendor 2 and the 300 μm thick resin from vendor 1. Besides, an increase of 7% was observed between the thin coated (20 μm thick) and the full encapsulated (150 μm thick) SiPM arrays from vendor 2. The resulting optimized performance suggested to pursue the thinner protective window solution.

3˙3. *Impact of sensor geometry*. – As mentioned, BTL sensors are designed to feature three different thicknesses along the pseudorapidity. A picture of three crystal arrays is reported in fig. 6, where they are shown from the thickest (on the left) to the thinnest (on the right). These three geometries are later referred to as type 1, type 2 and type 3, respectively.

In order to maintain approximately the same level of LCE in all module geometries, the SiPM active area is designed to match the crystal end face dimensions. It is assumed that for the considered crystal geometry, *i.e.*, a bar-like geometry, the photons reaching the SiPMs are primarily those that undergo total internal reflection inside the crystal volume and the LCE is assumed to scale linearly with the fraction of surface covered by the SiPM.

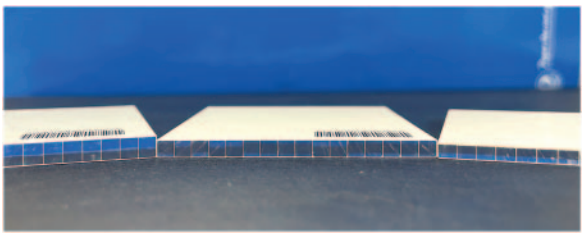

Fig. 6. – Picture of the three different LYSO array types. From left to right the type 1, type 2 and type 3 LYSO arrays are shown.

To evaluate the validity of the hypothesis, several light output measurements of different configurations were performed. Both LYSO and SiPM arrays from different vendors were tested in order to assess that results do not depend on the specific sensor considered. LYSO arrays from two specific vendors, later referred to as vendor A and vendor B, were coupled both to SiPM arrays from vendor 1 and vendor 2. It is worth mentioning that each LYSO array was first characterised at the University La Sapienza in Rome [6] and then delivered to Milano-Bicocca. Therefore each crystal array mentioned in this study was first measured there. According to those measurements, a spread in the light output of 5% was observed among samples from the same vendor and it was attributed to crystal-to-crystal difference in LY arising from small variations in the crystal growth process and composition of the raw materials. In order to factor out such differences from those due to the LCE, each light output value was normalized to the average light output of the samples from the same vendor measured in Rome as

$$LO_{normalized} = LO_{measured} \cdot \frac{\langle LO_{Rome} \rangle}{LO_{Rome}}. \tag{6}$$

Different geometries of LYSO arrays from a specific vendor were coupled to SiPMs both from vendor 1 and vendor 2 having the same dimensions of the crystal bar end face to which they were coupled. An increase in light output was observed for thicker modules compared to the thinner ones, as reported in fig. 7.

The same light output measurements were also performed on modules consisting of LYSO arrays from vendor B and SiPMs from both vendor 1 and vendor 2. It emerged the same trend for both vendors, with the light output increasing with the sensor thickness. This indicates that the resulting effect is independent of the specific crystal used.

The light output measured for each configuration is plotted as a function of the sensor geometries in fig. 8(left). An increase in the light output, thus of light collection efficiency, is observed for thicker crystals in each configuration: the LCE measured for the thickest sensors is greater than that of the thinnest sensors by up to 15%. Since scintillation photons are emitted isotropically inside the crystal volume, in crystals with a larger cross section (end face) the solid angle of photons reaching the SiPM without any reflection on the surfaces is larger. In addition, the average number of reflections of photons will be smaller thus increasing the probability for them to be detected.

Light output measurements were also performed on LYSO arrays coupled to SiPMs of different dimensions compared to the crystal bar end face in order to assess the potential effect of the sensor geometry on the LCE. Each SiPM geometry was coupled to crystals having different dimensions. The light output measured for the thickest SiPM is quite

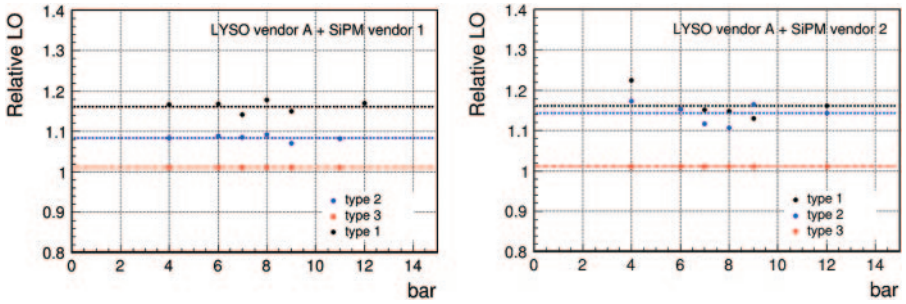

Fig. 7. – Relative comparison of the light output values measured for a set of bars of each module type. The results obtained for type 1, type 2 and type 3 modules are plotted with black, blue and red dots, respectively. Each light output value was normalized as reported in eq. (6) and divided to the results obtained for type-3 module in order to make a relative comparison. As an example, the light output performance of modules consisting of LYSO arrays from vendor A coupled to SiPM arrays from both vendor 1 (left) and 2 (right) are shown.

independent of the crystal thickness coupled to it. This can be explained considering that in each of the three tested configurations, the entire surface of the crystal end is covered by the active area of the SiPM and suggests that increasing the SiPM active area would not enhance the light output performance of the BTL modules.

On the other hand, SiPMs of type 2 and type 3 coupled to crystal bars of a different thickness show a decreasing trend as a function of the crystal thickness. This is due to the fact that the SiPM active area is smaller compared to the crystal bar end face and a fraction of the photons reaching the crystal end is not collected. Such an effect confirms the assumption that LCE scales linearly with the fraction of the crystal face covered with SiPM active area. This can be seen in fig. 8(right) where the light output measured in the different configurations is reported as a function of fraction of surface covered by the

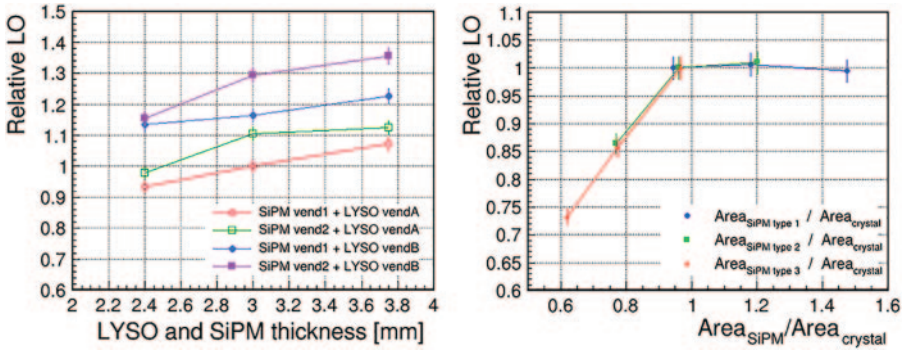

Fig. 8. – Left: a relative comparison between the light output of modules consisting of different combinations of SiPM and LYSO vendors is reported as a function of the module type. The relative comparison is made by normalizing each light output value to the one measured for the type 2 module made of a LYSO array from vendor A coupled to SiPM arrays from vendor 1. Right: light output as a function of the fraction of crystal surface covered by the SiPM active area is reported. The relative comparison is made by normalizing each light output value to the one measured for the module consisting of the same type sensors.

sensitive area of the SiPM. The light output scales linearly with the ratio of SiPM to crystal surface: there is a linear increase in LCE until the entire crystal surface is covered by the SiPM area.

4. – Conclusions and future perspectives

To address the challenges of HL-LHC in terms of pileup events, a new timing detector targeting a time resolution of 30–60 ps will be integrated in CMS. The MIP Timing Detector will provide accurate timing measurements that will enable the use of 4-dimensional vertexing improving the precision of the event reconstruction at HL-LHC and bringing new capabilities to the CMS experiment. The MTD will feature a hermetic coverage up to a pseudorapidity of $\eta = 3$ and will be constituted of two regions: the Barrel Timing Layer and the Endcap Timing Layer.

This study was focused on the characterization of BTL modules consisting of 16 elongated LYSO:Ce crystal bars coupled at both ends to SiPMs. To achieve the desired timing performance, the different terms contributing to the time resolution were identified and all of them depend on the light output, which resulted to be a key variable to optimize the time resolution of the detector.

A detailed study of BTL sensor modules performance in terms of light output using radioactive sources was performed in a laboratory in Milano-Bicocca. Aiming to enhance the light output of BTL modules, several tests were performed focusing on the optimization of the light collection efficiency.

A potential optimization of the LYSO array package was explored and consisted in removing the glue layer that was initially located between the crystals and the array wrapping. The resulting performance showed an improvement in light output thus leading to the definition of a new optimized packaging of LYSO arrays.

The results of the measurements performed on protective windows having different thicknesses drove to choose thinner resins for the SiPM production, which provide a better light output compared to thicker protective windows.

Finally, the impact of different sensor geometries on LO was evaluated. A drop of light output directly proportional to the fraction of crystal end face covered by a SiPM was measured and an increase in the light output as a function of the modules thickness was observed: thicker modules provided a higher LCE up to 15% compared to the thinnest ones. This effect was not taken into account in the original detector design and opens the possibility to improve the detector performance by thickening the crystals with a significant impact on time resolution. Thicker crystals, compared to thinner crystals, would indeed lead to both a higher energy deposited by the MIP crossing the crystal and a higher LCE. This would result in an improved performance, but it would also increase the production cost which needs to be carefully evaluated to assess the overall advantage yielded by thickening crystals.

In conclusion, the results of this study provided a comprehensive and thorough investigation of the design parameters which define the light output of a sensor module. This work offers a preliminary reference for the forthcoming assembly phase which requires stable and reproducible methods for light output measurements to assess the uniformity and the quality of a large amount of assembled modules during production. In particular, this first comparative study of the light output of different module geometries represents an important reference for the potential final optimization of the BTL design.

REFERENCES

[1] Apollinari G., Brüning O., Nakamoto T. and Rossi L., *High Luminosity Large Hadron Collider HL-LHC*, CERN yellow report CERN-2015-005, CERN, Geneva, Switzerland (2015).
[2] CMS Collaboration, *JINST*, **3** (2008) S08004.
[3] CMS Collaboration, *A MIP Timing Detector for the CMS Phase-2 Upgrade*, CERN technical report CERN-LHCC-2019-003, CERN, Geneva, Switzerland (2019).
[4] Albuquerque E. *et al.*, *TOFHIR2: The readout ASIC of the CMS Barrel MIP Timing Detector*, *IEEE Nuclear Science Symposium and Medical Imaging Conference (NSS/MIC)* (IEEE) 2020.
[5] Niknejad T. *et al.*, *Results with the TOFHIR2X revision of the front-end ASIC of the CMS MTD Barrel Timing Layer*, *IEEE Nuclear Science Symposium and Medical Imaging Conference (NSS/MIC)* (IEEE) 2021.
[6] Addesa F. M. *et al.*, *JINST*, **17** (2022) P08028.